[5] J. Bornemann, "Comparison between different formulations of the transverse field-matching technique for the three-dimensional analysis of metal-finned waveguide resonators," *Int. J. Numer. Model.*, vol. 4, pp. 63–73, Mar. 1991.
[6] V. A. Labay and J. Bornemann, "Matrix singular-value decomposition for pole-free solutions of homogeneous matrix equations as applied to numerical modeling methods," *IEEE Microwave Guided Wave Lett.*, vol. 2, pp. 49–51, Feb. 1992.
[7] U. Balaji and R. Vahldieck, "Radial mode matching analysis of ridged circular waveguides," *IEEE Trans. Microwave Theory Tech.*, vol. 44, pp. 1183–1186, July 1996.
[8] R. Behe and P. Brachat, "Compact duplexer-polarizer with semicircular waveguide," *IEEE Trans. Antennas Propagat.*, vol. 39, pp. 1222–1224, Aug. 1991.
[9] A. Elsherbeni, D. Kaifez and S. Zeng, "Circular sectoral waveguides," *IEEE Trans. Antennas Propagat.*, vol. 33, pp. 20–27, Dec. 1991.

An Application of FDTD in Studying the End Effects of Slotline and Coplanar Waveguide with Anisotropic Substrates

Jaideva C. Goswami and Raj Mittra

***Abstract*— In this paper, the finite-difference time-domain (FDTD) method is applied in conjunction with the generalized pencil of function (GPOF) technique to evaluate the reflection coefficient from shorted slotlines and coplanar waveguides (CPW) on anisotropic substrates, and to extract the propagation constant along the line from these data. For each frequency, the field solutions at different locations are processed by using the GPOF technique to extract two complex exponents that correspond to the forward and backward traveling waves, which provide all the information about the reflection coefficient and the dispersion characteristic of the transmission line. The advantage of combining the GPOF technique with the FDTD method is that the reflection coefficients can be obtained with a single run. Recognizing that there is a dearth of results for the reflection coefficients of slotline and CPW-line discontinuities with anisotropic substrates, the present problem is also solved by using the spectral-domain method for the purpose of validation, and the two results are found to compare quite well with each other. For further validation, the FDTD and GPOF solutions are derived for isotropic substrates, and are compared with the published theoretical and experimental results.**

***Index Terms*— CPW, FDTD method, GPOF method, SDA, slotline, transmission-line discontinuities.**

I. Introduction

One of the most challenging difficulties encountered in the design of microwave and millimeter-wave integrated circuits is to accurately characterize various kinds of transmission-line discontinuities. Although the literature is replete with theoretical and experimental research related to microstrip discontinuities, the same cannot be said about other types of transmission lines, e.g., coupled-microstrip lines, slot lines, and coplanar waveguides (CPW's). The end effects of a number of transmission-line structures have been discussed in [1], [2]. Some experimental results on slot lines have been reported in [3] and [4], and CPW's and slot lines have been the subjects of investigation in [5]–[15]. A number of papers related to CPW lines are contained in the September 1993 issue of IEEE TRANSACTIONS ON MICROWAVE THEORY AND TECHNIQUES. Muller *et al.* [8] have used the thru-line matrix (TLM) method to compute the inductance and virtual line length for a CPW short discontinuity. Dib *et al.* [10] have analyzed both open and shielded CPW discontinuities by using the space-domain integral-equation method. The mode-matching technique has been used by Rahman and Nguyen [14] to compute the S-parameters for three-layer step discontinuities. More recently, the finite-difference frequency-domain method has been employed in [15] for the analysis of CPW short circuits.

All of the above-mentioned literature has dealt with isotropic substrates—and the available results for anisotropic substrates are relatively few. In this paper, we analyze the slotline and CPW discontinuities on anisotropic substrates by using the full-wave finite-difference time-domain (FDTD) method, which enables us to obtain the characteristics of the discontinuities over a wide range of frequencies with a single run.

In the conventional approach of analyzing the discontinuities problems, an FDTD code is run twice, first for a continuous line and then in the presence of the discontinuity, to derive the time-domain fields for both the incident and reflected waves. In this paper, we combine the generalized pencil of function (GPOF) method with the FDTD method to compute the reflection coefficient in a single run. First, we obtain the field solutions over the desired frequency band at a number of equally spaced points located along the transmission line, and subsequently use the GPOF to extract two complex exponents for each frequency, which adequately represent the computed fields, and to extract the forward and backward traveling waves from these field data. The knowledge of the incident and reflected fields, in turn, yields the dispersion characteristics of the line as well as the reflection coefficient due to the discontinuity.

We use the cubic spline for the purpose of exciting the transmission line in the FDTD calculations. The time-frequency window product of the cubic spline is very close to 0.5—the lowest possible value that corresponds to Gaussian-type pulses—and the cubic spline has low-pass filter characteristics similar to the Gaussian. Consequently, for all practical purposes, the cubic spline is similar to the Gaussian and has the additional advantage of being compact in support, which in turn, avoids the need for truncation.

This paper is organized as follows. In the Section II, we discuss the FDTD solutions and their processing using the GPOF technique. To validate the FDTD/GPOF results, we also solve the present problem by using the spectral-domain analysis (SDA) which is briefly discussed in Section III. In Section IV, we discuss and compare the FDTD/GPOF and SDA results. For further validation, we apply the FDTD/GPOF to slotlines and CPW's with isotropic substrates, and compare our solutions with the published theoretical and experimental results. Finally, we present some conclusions in Section V to summarize our findings.

II. Finite-Difference Time-Domain Solution

The geometry of the problem to be studied in this paper is shown in Fig. 1. Although the figure shows the substrate with both the

Manuscript received June 11, 1996; revised April 2, 1997. This work was supported in part by the Joint Services Electronics Program under Grant N00014-96-1-0129 and in part by a Summa Foundation Fellowship.

J. C. Goswami was with the Electromagnetic Communication Laboratory, Department of Electrical and Computer Engineering, University of Illinois at Urbana-Champaign, IL 61801 USA. He is now with Schlumberger Wireline and Testing, Sugar Land, TX 77478 USA.

R. Mittra was with the Electromagnetic Communication Laboratory, Department of Electrical and Computer Engineering, University of Illinois at Urbana-Champaign, IL 61801 USA. He is now with the Department of Electrical Engineering, Pennsylvania State University, University Park, PA 16802 USA.

Publisher Item Identifier S 0018-9480(97)06074-2.

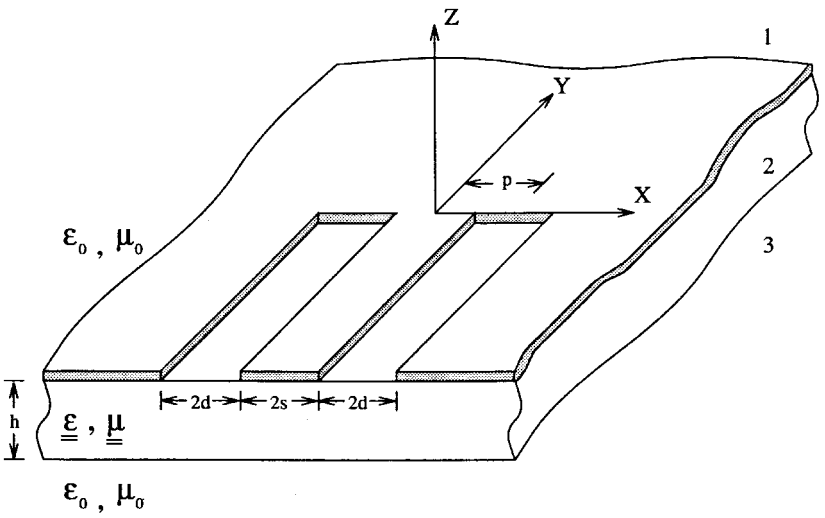

Fig. 1. Short-circuited CPW.

electric and magnetic anisotropies (and our solution technique can accommodate these general cases), we restrict ourselves in this paper to the presentation of results for electrically anisotropic substrates only. For these substrates, we can represent the relative permittivity tensors in the form

$$\underline{\underline{\epsilon}} = \underline{\underline{I}}_t \epsilon_t + \hat{z}\hat{z}\epsilon_z \tag{1}$$

where $\underline{\underline{I}}_t$ is the identity dyadic, transverse to the optic axis $\hat{z}$.

Next, we apply the FDTD method to obtain the E_x and H_z fields at a number of points along the transmission line. While the knowledge of only one of the field components is sufficient for the present analysis, we evaluate both these field components for the purpose of understanding the field behavior near the discontinuity. For each geometry, the number of cells along x (N_x), y (N_y), and z (N_z) are 55, 190, and 45, respectively. The corresponding spatial discretizations Δ_x, Δ_y, and Δ_t, as well as the time discretization Δ_t will be detailed in Section IV. The computational domain is truncated by placing first-order Mur absorbing boundaries at $y = 0$ and $y = N_y\Delta_y$, and using second-order Mur boundaries along the other directions. The simulation is run for 3000 time steps.

The transmission lines are excited by using a cubic spline pulse for the E_x fields in the slot regions at the cell location 20 along the y-axis and at the air-dielectric interface. The discontinuity is located at $y = 170\Delta_y$. In the CPW, the even mode is simulated by exciting the two slots with pulses having the same amplitude and sign, whereas in the case of an odd mode, the sign of one of the pulses is reversed.

The cubic spline (ϕ_C), and more precisely the cardinal cubic B-spline, is defined as

$$6\phi_C(t) := \begin{cases} t^3, & t \in [0,1] \\ 4 - 12t + 12t^2 - 3t^3, & t \in [1,2] \\ -44 + 60t - 24t^2 + 3t^3, & t \in [2,3] \\ 64 - 48t + 12t^2 - t^3, & t \in [3,4] \end{cases} \tag{2}$$

with its Fourier transform $\hat{\phi}_C$ given by

$$|\hat{\phi}_C(\omega)| = \left(\frac{\sin(\omega/2)}{\omega/2}\right)^4. \tag{3}$$

For a given 3-dB frequency f_0, we need to scale the cubic spline given in (2) by a factor of R, where $R = 4.402\,7649 f_0$. For the same 3-dB frequency, the Gaussian pulse is given by

$$\phi_G(t) = \exp\left[-\left(\frac{t-T}{0.29T}\right)^2\right] \tag{4}$$

with $T = 0.646/f_0$.

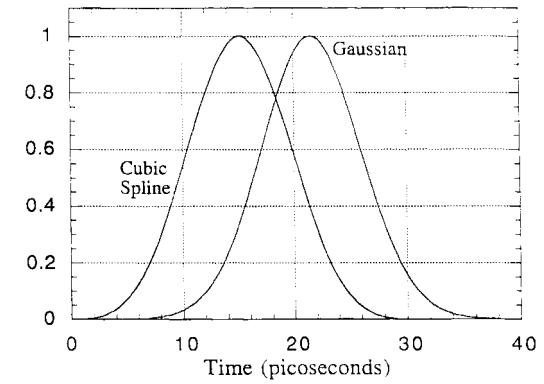

(a)

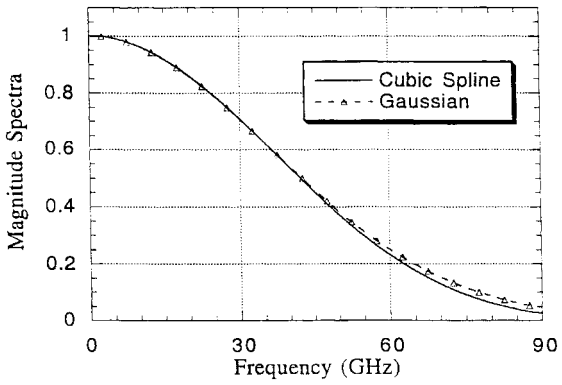

(b)

Fig. 2. Cubic spline and Gaussian pulses in (a) time domain and (b) frequency domain.

The time–frequency–window product (see [16, p. 7] for the definition of the window width) of the cubic spline is 0.501, which is very close to 0.5, the lowest possible value that corresponds to Gaussian-type windows. In Fig. 2, we show the cubic spline and the Gaussian pulses, along with their magnitude spectra for the 3-dB frequency of 30 GHz. It is evident from Fig. 2 that the time-frequency characteristics of the two are quite similar; however, in contrast to the Gaussian, the cubic spline requires no truncation.

The next step in our procedure is to process the field solutions by using the GPOF algorithm [17], [18]. From a set of discrete data

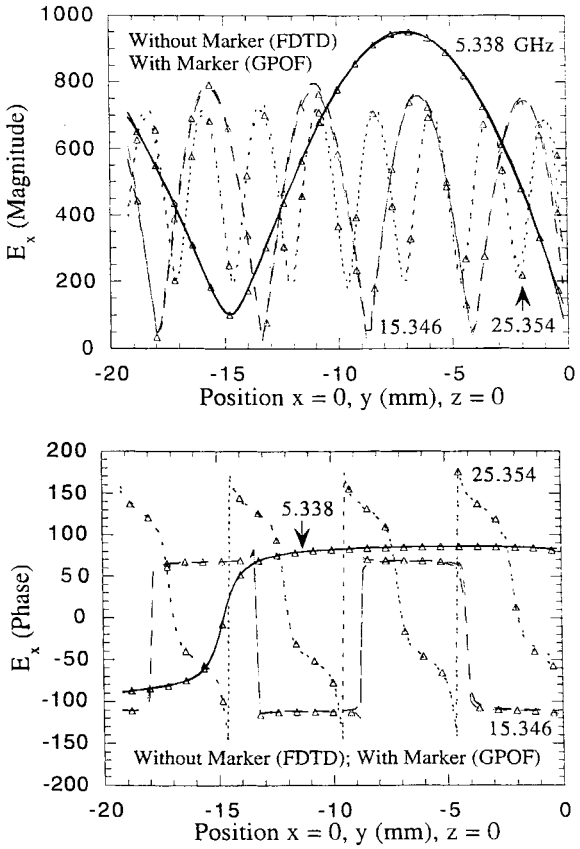

Fig. 3. Comparison of the FDTD solutions for the electric field in the slot of a slotline on sapphire substrate with their approximations using two complex exponents extracted from the FDTD solutions by using the GPOF.

$\{f_i\colon i = 0, \cdots, M\}$ of a complex valued function f, this algorithm finds the complex coefficients $\{c_i, \gamma_i\colon i = 1, \cdots, N\}$ such that

$$f_i := f(x_i) = \sum_{k=1}^{N} c_k \ \exp(\gamma_k x_i), \qquad N < M \tag{5}$$

where $x_i = i\Delta_x$ and Δ_x is the discretization step. While the GPOF technique is similar to the Prony's method [19], the difference between the two lies in the manner in which the complex poles are extracted.

The FDTD solutions for E_x are compared with the GPOF results with two complex exponents in Fig. 3, and the two results agree quite well. Although the lines are lossless, the real parts of γ_i still have some small nonzero values that are numerical artifacts. The imaginary parts of γ_i yield the propagation constants, whereas the relative magnitudes of the coefficients c_i correspond to the reflection coefficients.

III. Spectral-Domain Analysis (SDA)

To verify the FDTD results we re-solve the discontinuities problems shown in Fig. 1 by using the spectral-domain method, which is briefly discussed below.

The time-harmonic forms of the Maxwell's equation for an anisotropic medium are given by

$$-\nabla \times \boldsymbol{E} = j\omega \ \mu_0 \ \underline{\underline{\boldsymbol{\mu}}} \cdot \boldsymbol{H} + \boldsymbol{M} \tag{6}$$

$$\nabla \times \boldsymbol{H} = j\omega \ \epsilon_0 \ \underline{\underline{\boldsymbol{\epsilon}}} \cdot \boldsymbol{E} + \boldsymbol{J}. \tag{7}$$

We can obtain the dyadic magnetic-field Green's functions $\underline{\underline{\boldsymbol{G}}}^{HM}(\boldsymbol{r}, \boldsymbol{r}')$ from (6) and (7) in terms of the transmission-line Green's function [20, ch. 2]. A detailed description of such a formulation can be found in [21], [22].

Observe that the CPW reduces to a slotline if we let $p = 0$ in Fig. 1. In the present analysis, we first separate the problem of Fig. 1(b) into two parts by invoking the equivalence principle [23], which enables us to replace the slot regions by equivalent surface magnetic current, viz.

$$\boldsymbol{M}_s(\boldsymbol{r}) = \boldsymbol{E}(\boldsymbol{r}) \times \hat{z}; \quad \boldsymbol{r} \in \mathcal{D} := \mathcal{D} + \cup\mathcal{D}^- \tag{8}$$

where $\mathcal{D}^+ := \{x, y, z | x \in (s, s + 2d), y \in (-\infty, 0], z = 0\}$ and $\mathcal{D}^- := \{x, y, z | x \in (-s, -s - 2d), y \in (-\infty, 0], z = 0\}$. We then obtain the magnetic-field integral equation by enforcing the boundary condition

$$\hat{z} \times \boldsymbol{H}(\boldsymbol{r}) = 0, \qquad \boldsymbol{r} \in \mathcal{D}. \tag{9}$$

We assume that the slotwidth is very small compared to the operating wavelength and, therefore, we consider only the y-component of the magnetic field. With the suitable basis functions for the magnetic field satisfying the appropriate edge conditions, we arrive at the following equation:

$$\int_{-\infty}^{\infty} \int_{-\infty}^{\infty} \Lambda^{HM}(k_x, k_y) \hat{f}_y(k_y) \hat{\phi}_k(-k_y) \ dk_x \ dk_y = 0 \tag{10}$$

where

$$\Lambda^{HM}(k_x, k_y) = \hat{G}_{yy}^{HM}(k_x, k_y) J_0^2(k_x d) \begin{Bmatrix} \cos^2(k_x p) \\ \sin^2(k_x p) \end{Bmatrix} \tag{11}$$

with $\cos^2(k_x p)$ and $\sin^2(k_x p)$ for even and odd modes, respectively. In (10), $\hat{f}_y(k_y)$ and $\hat{\phi}_k(k_y)$ are the Fourier transforms of the basis functions representing y-dependence of the magnetic current. To find the propagation constant, k_{ye} of an infinite transmission line, we assume that the y-dependence of all the field and current distributions is given by $e^{-jk_{ye}y}$. For this case, we arrive at a simple equation for the determination of k_{ye}, that reads

$$\int_{-\infty}^{\infty} \Lambda^{HM}(k_x, k_{ye}) \ dk_x = 0. \tag{12}$$

For the longitudinal variation of the magnetic current, we consider

$$f_y(y) = s_i(y) + \Gamma s_r(y) + \sum_{k=0}^{K} c_k \phi_k(y) \tag{13}$$

where $K > 0$. Although $|\Gamma|$, the magnitude of the reflection coefficient should be unity for a shorted line, it turns out to be somewhat less than one because of the nonideal nature of the terminations shown in Fig. 1. The expressions for the entire domain functions s_i, s_r, and the sub-domain basis functions ϕ_k may be found in [24], [25]. Finally, we use the above functions also as testing functions and apply the Galerkin procedure to obtain a set of linear equations, whose solution yields the desired results for the reflection coefficient Γ.

IV. Numerical Results and Discussions

All of the FDTD results in this paper have been obtained by using the decretizations $\Delta_x = \Delta_y = \Delta_z = 0.0002$ m, and $\Delta_t = 0.365\,908\,3$ ps, except for the ones in Fig. 6, where we have used $\Delta_x = \Delta_y = \Delta_z = 0.000\,16$ m, and $\Delta_t = 0.292\,726\,6$ ps. The various integrals involved in the SDA have been evaluated by performing the integrations along the real axis. A major observation regarding the locations of the surface-wave poles is that, unlike the case of an isotropic substrate, the TE and TM poles may not alternate

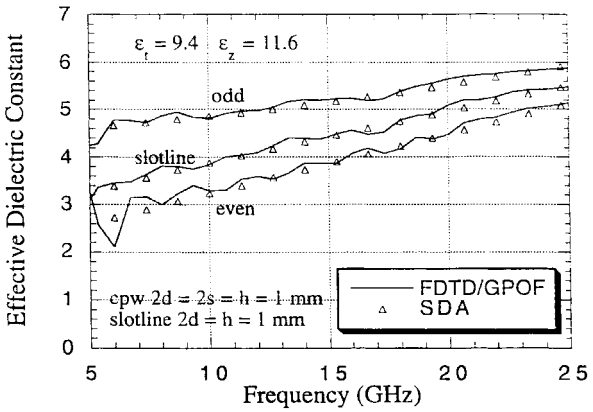

Fig. 4. Effective dielectric constants of slotline and CPW by using the FDTD/GPOF and SDA methods.

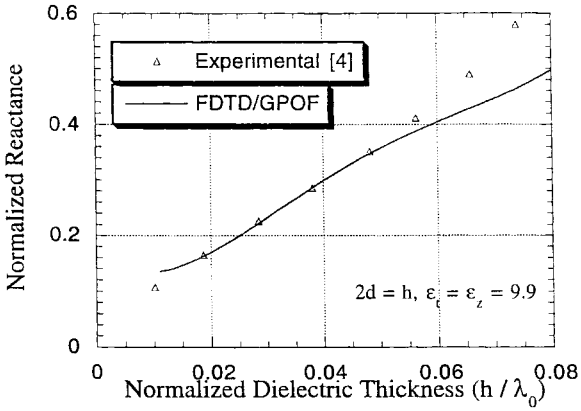

Fig. 5. Comparison of the FDTD/GPOF solution with the experimental result in [4] for the normalized reactance of a shorted slotline.

for anisotropic substrates. The details on the surface-wave poles and residues may be found in [22].

In Fig. 4, the FDTD/GPOF results for effective dielectric constants for the slotline and the CPW on sapphire substrate ($\epsilon_t = 9.4, \epsilon_z = 11.6$) are compared with those derived by using the SDA, and are seen to agree very well with each other. In plotting the FDTD/GPOF solutions in Figs. 5–8, we have applied a smoothing procedure to eliminate the numerical artifacts. In Figs. 5 and 6, we compare the FDTD/GPOF solutions with the experimental [4] and theoretical [11] results for the alumina substrate ($\epsilon_t = \epsilon_z = 9.9$). Figs. 7 and 8 compare the results for the magnitude and phase of the reflection coefficients of the slotline and the CPW obtained by using the FDTD/GPOF and the spectral-domain analyses. We note that the discrepancies between the solutions become significant at higher frequencies where the SDA results may not be very accurate because of the various assumptions about the slotwidth and the basis functions made in the SDA.

V. Conclusions

In this paper, we have combined the FDTD method for electromagnetic-field computation with the GPOF technique, which extracts the complex poles from the field data, and have applied this combination to analyze the short-circuit discontinuities in the slotlines and the CPW's. We have demonstrated the effectiveness of the method by computing the reflection coefficient from the field solutions obtained from a single run of the FDTD simulation, as opposed to the conventional two-step process. We have also shown

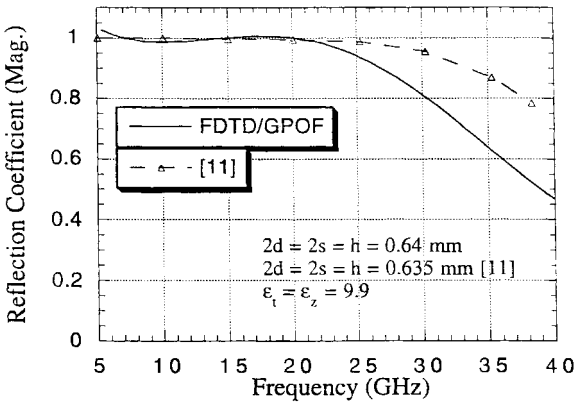

Fig. 6. Comparison of the FDTD/GPOF solution for the magnitude of the reflection coefficient of a shorted CPW with the theoretical result in [11].

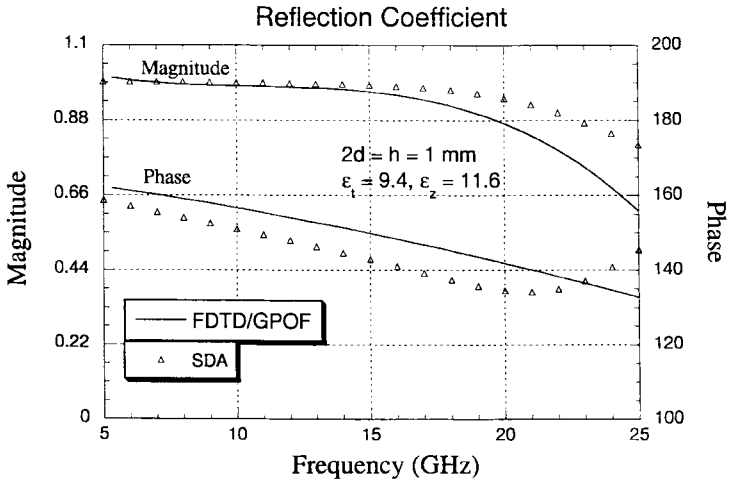

Fig. 7. Reflection coefficient for a shorted slotline on sapphire substrate.

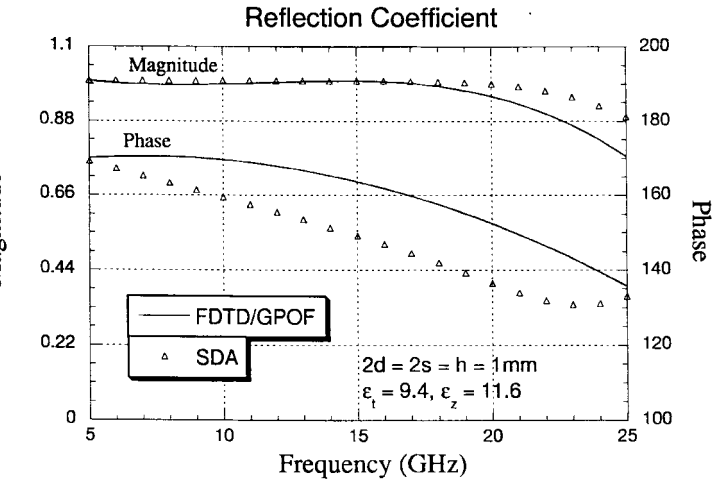

Fig. 8. Reflection coefficient for a shorted CPW on sapphire substrate.

that the cubic-spline excitation is similar to the Gaussian, but has the advantage over the latter in that it requires no truncation. We have validated our results by comparing them with the theoretical and experimental data from other sources.

References

[1] R. H. Jansen, "Hybrid mode analysis of end effects of planar microwave and millimeter wave transmission lines," *Proc. Inst. Elect. Eng.*, vol. 128, pt. H, pp. 77–86, Apr. 1981.

[2] R. H. Jansen and N. H. L. Koster, "Accurate results on the end effect of single and coupled microstrip lines for use in microwave circuit design," *Arch. Elektron. Über. (AEÜ)*, vol. 34, pp. 453–459, 1980.
[3] J. B. Knorr and J. Saenz, "End effect in a shorted slot," *IEEE Trans. Microwave Theory Tech.*, vol. MTT-21, pp. 579–580, Sept. 1973.
[4] J. Chramiec, "Reactance of slotline short and open circuits on alumina substrate," *IEEE Trans. Microwave Theory Tech.*, vol. 37, pp. 1638–1641, Oct. 1989.
[5] H. Y. Yang and N. G. Alexópoulos, "A dynamic model of microstrip-slotline transition and related structures," *IEEE Trans. Microwave Theory Tech.*, vol. 36, pp. 286–293, Feb. 1988.
[6] R. W. Jackson, "Mode conversion at discontinuities in finite-width conductor-backed coplanar waveguide," *IEEE Trans. Microwave Theory Tech.*, vol. 37, pp. 1582–1589, Oct. 1989.
[7] G. Bartolucci and J. Piotrowski, "Full-wave analysis of shielded coplanar waveguide short-end," *Electron. Lett.*, vol. 26, pp. 1615–1616, Sept. 1990.
[8] U. Muller, M. Rittweger, and A. Beyer, "Coplanar short considered by the TLM-method with symmetrical condensed nodes," in *IEEE European Microwave Conf.*, Stuttgart, Germany, Sept. 1991, pp. 999–1003.
[9] M. Drissi, V. F. Hanna, and J. Citerne, "Analysis of coplanar waveguide radiating end effects using the integral equation technique," *IEEE Trans. Microwave Theory Tech.*, vol. 39, pp. 112–116, Jan. 1991.
[10] N. I. Dib, W. P. Harokopus, Jr., G. E. Ponchak, and L. P. B. Katehi, "A comparative study between shielded and open coplanar waveguide discontinuities," *Int. J. Microwave Millimeter-Wave Computer-Aided Eng.*, vol. 2, pp. 331–341, 1992.
[11] J. S. Mclean, A. D. Wieck, K. Ploog, and T. Itoh, "Full-wave analysis of open-end discontinuities in coplanar stripline and finite ground plane coplanar waveguide in open environments using a deterministic spectral domain approach," in *IEEE European Microwave Conf.*, Stuttgart, Germany, Sept. 1991, pp. 1004–1007.
[12] C. W. Chiu and R. B. Wu, "A moment method analysis for coplanar waveguide discontinuity inductances," *IEEE Microwave Theory Tech.*, vol. 41, pp. 1511–1514, Sept. 1993.
[13] A. M. Tran and T. Itoh, "Full-wave modeling of coplanar waveguide discontinuities with finite conductor thickness," *IEEE Microwave Theory Tech.*, vol. 41, pp. 1611–1615, Sept. 1993.
[14] K. R. Rahman and C. Nguyen, "On the analysis of single- and multiple-step discontinuities for a shielded three-layer coplanar waveguide," *IEEE Trans. Microwave Theory Tech.*, vol. 41, pp. 1484–1488, Sept. 1993.
[15] H. Klingbeil, K. Beilenhoff, and H. L. Hartnagel, "FDTD full-wave analysis and modeling of dielectric and metallic losses of CPW short circuits," *IEEE Trans. Microwave Theory Tech.*, vol. 44, pp. 485–487, Mar. 1996.
[16] C. K. Chui, *An Introduction to Wavelet*. Norwood, MA: Academic, 1992.
[17] A. J. Mackay and A. McCowen, "An improved pencil-of-function method and comparisons with traditional methods of pole extraction," *IEEE Trans. Antennas Propagat.*, vol. AP-35, pp. 435–441, Apr. 1987.
[18] Y. Hua and T. K. Sarkar, "Generalized pencil-of-function method for extracting poles of an EM system from its transient response," *IEEE Trans. Antennas Propagat.*, vol. 37, pp. 229–234, Feb. 1989.
[19] M. L. Van Blaricum and R. Mittra, "Problem and solutions associated with Prony's method for processing transient data," *IEEE Trans. Antennas Propagat.*, vol. AP-26, pp. 174–182, Jan. 1978.
[20] L. B. Felsen and N. Marcuvitz, *Radiation and Scattering of Waves*. Piscataway, NJ: IEEE Press, 1994.
[21] K. A. Michalski, "Formulation of mixed-potential integral equations for arbitrarily shaped microstrip structures with uniaxial substrate," *J. Electromagnetic Waves Appl.*, vol. 7, pp. 899–917, 1993.
[22] J. C. Goswami, "Applications of semi-orthogonal spline wavelets in electromagnetics and microwave problems," Ph.D. dissertation, Texas A&M University, College Station, Aug. 1995.
[23] R. F. Harrington, *Time-Harmonic Electromagnetic Fields*. New York: McGraw-Hill, 1961.
[24] T. S. Horng, N. G. Alexópoulos, S. C. Wu, and H. Y. Yang, "Full-wave spectral-domain analysis for open microstrip discontinuities of arbitrary shape including radiation and surface-wave losses," *Int. J. Microwave Millimeter-Wave Computer-Aided Eng.*, vol. 2, pp. 224–240, 1992.
[25] J. C. Goswami, A. K. Chan, and C. K. Chui, "Spectral-domain analysis of single and coupled microstrip open discontinuities with anisotropic substrates," *IEEE Trans. Microwave Theory Tech.*, vol. 44, pp. 1174–1178, July 1996.